(195)
60-07-05

DP-1540

MODELING PRINCIPLES APPLIED TO THE SIMULATION OF A JOULE-HEATED GLASS MELTER

KENNETH R. ROUTT

E. I. du Pont de Nemours & Co.
Savannah River Laboratory
Aiken, SC 29808

PREPARED FOR THE U. S. DEPARTMENT OF ENERGY UNDER CONTRACT DE-AC09-76SR00001

Printed in the United States of America
Available from

National Technical Information Service
U. S. Department of Commerce
5285 Port Royal Road
Springfield, Virginia 22161

Price: Printed Copy A03; Microfiche A01

DP-1540
Distribution Category UC-38

MODELING PRINCIPLES APPLIED TO THE SIMULATION OF A JOULE-HEATED GLASS MELTER

Kenneth R. Routt

Approved by

J. A. Kelley, Research Manager

Publication Date: May 1980

E. I. du Pont de Nemours & Co.
Savannah River Laboratory
Aiken, SC 29808

PREPARED FOR THE U. S. DEPARTMENT OF ENERGY UNDER CONTRACT DE-AC09-76SR00001

726243r

ABSTRACT

Three-dimensional conservation equations applicable to the operation of a joule-heated glass melter were rigorously examined and used to develop scaling relationships for modeling purposes.

By rigorous application of the conservation equations governing transfer of mass, momentum, energy, and electrical charge in three-dimensional cylindrical coordinates, scaling relationships were derived between a glass melter and a physical model for the following independent and dependent variables:

- Geometrical size (scale)
- Velocity
- Temperature
- Pressure
- Mass input rate
- Energy input rate
- Voltage
- Electrode current
- Electrode current flux
- Total power
- Electrical resistance.

The scaling relationships were then applied to the design and construction of a physical model of the semiworks glass melter for the Defense Waste Processing Facility.

The design and construction of such a model using glycerine plus LiCl as a model fluid in a one-half-scale Plexiglas® tank is described.

® Trademark of Rohm and Haas Company.

CONTENTS

LIST OF FIGURES

LIST OF TABLES

MODELING PRINCIPLES APPLIED TO THE SIMULATION OF A JOULE-HEATED GLASS MELTER

INTRODUCTION

A key step in the reference process of converting liquid radioactive waste at the Savannah River Plant into an immobile glass product is the design and successful operation of a glass melter in which the waste and glass forming materials (frit) are mixed at high temperatures to form a homogeneous glass.

The high temperature (1150°C) of the melter makes it difficult to determine important data regarding the behavior of the glass within the melter. For example, there is no known technique which enables one to quantify the motion of the glass (velocity profiles) in the melter, but these profiles affect the homogeneity of the glass product. The use of tracer particles in a properly scaled, transparent model fluid can have a significant impact on understanding and design optimization of the melter.

Similarly, it is both difficult and uneconomical to experiment with electrode geometry, placement, and electrical phasing of applied electrode potential in an operating melter. But, again these effects as well as others, such as electrode current flux and the location of hot and cold spots, may all be assessed in a properly scaled model.

With this information in mind, the theoretical relationships necessary to design, operate, and interpret data from a glass melter model are developed and applied as an example to the semi-works full-scale melter operated as part of the research and development program for the Defense Waste Processing Facility. Data from the modeling program will be issued in a separate report.

I. THEORETICAL BASIS FOR SCALING

To relate model behavior to full-scale equipment, it is necessary to have a sound basis for scaleup of model data. This is achieved through the use of dimensional analysis based upon rigorous application of conservation equations.

1. Conservation of Mass, Momentum, and Energy

To derive the necessary scaling relationships for modeling a glass melter, first consider conservation of mass, momentum, and energy in three-dimensional, cylindrical coordinates (Figure 1), where

R = radius of melt chamber, and

Z = height of glass surface above the bottom of the melt chamber.

The steady state conservation of mass equation for a fluid can be written as[1]

$$\frac{1}{r}\frac{\partial}{\partial r}(\rho_o r v_r) + \frac{1}{r}\frac{\partial}{\partial \theta}(\rho_o v_\theta) + \frac{\partial}{\partial z}(\rho_o v_z) + W = 0 \qquad (1.1\text{-}1)$$

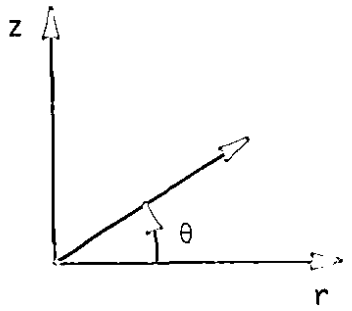

$0 \le r \le R$

$0 \le \theta \le 2\pi$

$0 \le z \le Z$

FIGURE 1. Coordinate System

where

ρ_o = fluid density* evaluated at temperature T_o

---

* The fluid density will change only slightly over the temperature range of interest. Evaluating it at a fixed temperature makes it constant in (1.1-1) and leads to considerable mathematical simplification.

v_r, v_θ, v_z = fluid velocities in the r, θ, and z directions, respectively, and

W = mass injection rate.

The steady-state r-component of the conservation of the momentum equation can be written as[1]

$$\rho_o\left(v_r\frac{\partial v_r}{\partial r}+\frac{v_\theta}{r}\frac{\partial v_r}{\partial\theta}-\frac{v_\theta^2}{r}+v_z\frac{\partial v_r}{\partial z}\right)=-g_o\frac{\partial p}{\partial r}$$
$$+\frac{\partial}{\partial r}\left[\frac{\mu}{r}\frac{\partial}{\partial r}(rv_r)\right]+\frac{1}{r^2}\frac{\partial^2(\mu v_r)}{\partial\theta^2}-\frac{2}{r^2}\frac{\partial(\mu v_\theta)}{\partial\theta}+\frac{\partial^2(\mu v_r)}{\partial z^2} \qquad (1.1\text{-}2)$$

The θ-component is

$$\rho_o\left(v_r\frac{\partial v_\theta}{\partial r}+\frac{v_\theta}{r}\frac{\partial v_\theta}{\partial\theta}+\frac{v_r v_\theta}{r}+v_z\frac{\partial v_\theta}{\partial z}\right)=\frac{-g_o}{r}\frac{\partial p}{\partial\theta}$$
$$+\frac{\partial}{\partial r}\left[\frac{1}{r}\frac{\partial}{\partial r}(r\mu v_\theta)\right]+\frac{1}{r^2}\frac{\partial^2(\mu v_\theta)}{\partial\theta^2}+\frac{2}{r^2}\frac{\partial(\mu v_r)}{\partial\theta}+\frac{\partial^2(\mu v_\theta)}{\partial z^2} \qquad (1.1\text{-}3)$$

The z-component is

$$\rho_o\left(v_r\frac{\partial v_z}{\partial r}+\frac{v_\theta}{r}\frac{\partial v_z}{\partial\theta}+v_z\frac{\partial v_z}{\partial z}\right)=-g_o\frac{\partial p}{\partial z}$$
$$+\frac{1}{r}\frac{\partial}{\partial r}\left[r\frac{\partial(\mu v_z)}{\partial r}\right]+\frac{1}{r^2}\frac{\partial^2(\mu v_z)}{\partial\theta^2}+\frac{\partial^2(\mu v_z)}{\partial z^2}+F_B \qquad (1.1\text{-}4)$$

where

μ = viscosity

p = pressure

F_B = body force

g_o = 32.14 lbm - ft/lbf-sec^2

The body force, F_B, is actually a buoyant force which arises due to density differences within the fluid. Although relatively small, it is the main driving force for fluid movement in the glass melter. Its magnitude can be determined as follows.

Let the volume element in Figure 2 be submerged in a fluid whose surface is at z = Z. The force on the top face of

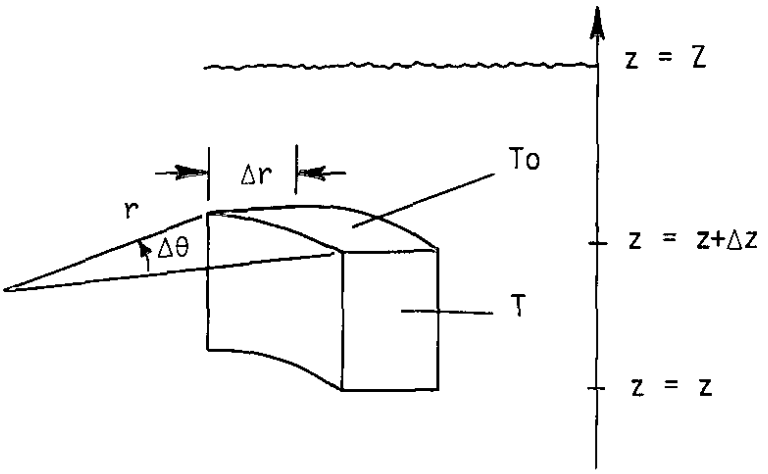

FIGURE 2. Submerged Volume Element

the volume element is

$$F_{top} = -\rho_o r\Delta\theta\Delta r\ [Z-(z+\Delta z)]g \qquad (1.1\text{-}5)$$

where

g = local gravitational constant

The force on the bottom face is

$$F_{bott} = F_{top} - \rho_o\ [1-\beta(T-T_o)]\ r\Delta\theta\Delta r\Delta z g \qquad (1.1\text{-}6)$$

where

T_o = temperature on the top face of the volume element

T = temperature of the fluid in the volume element

β = volumetric coefficient of expansion of the fluid.

The net body force F_B per unit volume is then

$$F_B\ r\Delta\theta\Delta r\Delta z = F_{bott} - F_{top}$$

$$= -\rho_o\ [1-\beta(T-T_o)]\ r\Delta\theta\Delta r\Delta z g \qquad (1.1\text{-}7)$$

or

$$F_B = -\rho_o g\ [1-\beta(T-T_o)] \qquad (1.1\text{-}8)$$

To uniquely specify a solution to the conservation of mass and momentum equations, apply the following boundary conditions for an axially symmetric case

$$v_r(R,\theta,z) = v_\theta(R,\theta,z) = v_z(r,\theta,Z) = v_z(r,\theta,0) = 0$$

$$\frac{\partial v_r(o,\theta,z)}{\partial r} = \frac{\partial v_\theta(0,\theta,z)}{\partial \theta} = 0$$

$$p(r,\theta,Z) = 0 \qquad (1.1\text{-}9)$$

The above boundary conditions are automatically satisfied in the model and in the melter by the presence of side-walls, a bottom, and atmospheric pressure at the surface of the fluid.

The equation for conservation of energy can be written as[1]

$$\rho_o c_{po}\left(v_r \frac{\partial T}{\partial r} + \frac{v_\theta}{r}\frac{\partial T}{\partial \theta} + v_z \frac{\partial T}{\partial z}\right) = \frac{1}{r}\frac{\partial}{\partial r}\left(rk \frac{\partial T}{\partial r}\right)$$

$$+ \frac{1}{r^2}\frac{\partial^2 (kT)}{\partial \theta^2} + \frac{\partial^2 (kT)}{\partial z^2} + Q \qquad (1.1\text{-}10)$$

where

c_{po} = specific heat of fluid evaluated at T_o

T = temperature

k = thermal conductivity of fluid

Q = energy input rate

The boundary conditions for (1.1-10) are

$$-k \frac{\partial T(R,\theta,z)}{\partial r} = U_{wall}\,[T(R,\theta,z) - T(R+\varepsilon,\theta,z)]$$

$$\frac{\partial T(0,\theta,z)}{\partial r} = \frac{\partial T(0,\theta,z)}{\partial \theta} = 0$$

$$T(0,0,Z/2) = T_{bulk}$$

$$-k \frac{\partial T(r,\theta,0)}{\partial z} = U_{bott}\,[T(r,\theta,0) - T(r,\theta,-\gamma)]$$

$$-k \frac{\partial T(r,\theta,Z)}{\partial z} = \left(\frac{q}{A}\right)_{feed} \qquad (1.1\text{-}11)$$

where

U_{wall}, U_{bott} = heat transfer coefficients of melter wall and bottom, respectively

ε = melter wall thickness

γ = melter bottom thickness

T_{bulk} = operating temperature of melter

$(q/A)_{feed}$ = heat flux at melter surface (a function of feedrate).

The second condition implies axial symmetry. These boundary conditions are not automatically satisfied by geometric similarity between the model and the melter, and thus require careful consideration during model design and operation.

To write the conservation equations in dimensionless form, define

$$r^* = c_r r \qquad \theta^* = c_\theta \theta \qquad z^* = c_z z$$

$$v_r^* = c_{vr} v_r \qquad v_\theta^* = c_{v\theta} c_\theta \qquad v_z^* = c_{vz} v_z$$

$$p^* = c_p' p \qquad T^* = c_t T \qquad W^* = c_w W$$

$$Q^* = c_q Q \qquad (1.1\text{-}12)$$

where the constants c_r, c_z, etc. are to be determined in such a manner that r*, z*, etc. become dimensionless, i.e., pure numbers.

If equations (1.1-12) are substituted into the five conservation equations [(1.1-1), (1.1-2),(1.1-3),(1.1-4),(1.1-10)] in an effort to solve for the c_r, c_z, etc., one finds that there are ten unknowns, but only five equations. This can be partially resolved by choosing

$$r^* = \frac{r}{R} \qquad \theta^* = \theta \qquad z^* = \frac{z}{R} \qquad (1.1\text{-}13)$$

Furthermore, if (1.1-12) is substituted into the momentum equations, products of $c_{v\theta}$ c_{vr}, c_{vz} c_{vr}, etc. will result. This suggests the following simplification. Let

$$c_{vr} = c_{v\theta} = c_{vz} = c_v \qquad (1.1\text{-}14)$$

The use of (1.1-13) and (1.1-14) reduces the scope of the problem to determination of c_v, c_p, c_t, c_w, and c_q. The energy equation (1.1-10) can now be written as

$$\frac{\rho_o c_{po}}{c_v c_t R}\left[v_r^* \frac{\partial T^*}{\partial r^*} + \frac{v_\theta^*}{r^*}\frac{\partial T^*}{\partial \theta^*} + v_z^* \frac{\partial T^*}{\partial z^*}\right]$$

$$= \frac{k_o}{R^2 c_t}\left\{\frac{1}{r^*}\frac{\partial}{\partial r^*}\left[r^*\left(\frac{k}{k_o}\right)\frac{\partial T^*}{\partial r^*}\right] + \frac{1}{r^{*2}}\frac{\partial^2}{\partial \theta^{*2}}\left[\left(\frac{k}{k_o}\right)T^*\right]\right.$$

$$\left. + \frac{\partial^2}{\partial z^{*2}}\left[\left(\frac{k}{k_o}\right)T^*\right]\right\} + \frac{Q^*}{c_q} \qquad (1.1\text{-}15)$$

To make (1.1-15) dimensionless, multiply through by

$$\frac{c_v c_t R}{\rho_o c_{po}}$$

and set

$$\frac{c_v c_t R}{\rho_o c_{po}} \times \frac{k_o}{R^2 c_t} = 1 \qquad (1.1\text{-}16)$$

which gives

$$c_v = \frac{\rho_o c_{po} R}{k_o} = \frac{R}{\alpha_o} \qquad (1.1\text{-}17)$$

where α_o = thermal diffusivity of the fluid. In equation (1.1-15) one must also set

$$\frac{c_v c_t R}{\rho_o c_{po}} \times \frac{1}{c_q} = 1 \qquad (1.1\text{-}18)$$

Having determined c_v, one must first determine c_t before (1.1-18) can be used to determine c_q.

Using (1.1-13) and (1.1-14) in the z-component of the momentum equation (1.1-4) gives

$$\frac{\rho_o}{c_v^2 R}\left[v_r^* \frac{\partial v_z^*}{\partial r^*} + \frac{v_\theta^*}{r^*}\frac{\partial v_z^*}{\partial \theta^*} + v_z^* \frac{\partial v_z^*}{\partial z^*}\right] = \frac{-g_o}{c_p R}\frac{\partial p^*}{\partial z^*}$$

$$+ \frac{\mu_o}{R^2 c_v}\left\{\frac{1}{r^*}\frac{\partial}{\partial r^*}\left[r^*\frac{\partial}{\partial r^*}\left(\frac{\mu}{\mu_o}v_z^*\right)\right] + \frac{1}{r^{*2}}\frac{\partial^2}{\partial \theta^{*2}}\left(\frac{\mu}{\mu_o}v_z^*\right)\right.$$

$$\left. + \frac{\partial^2}{\partial z^{*2}}\left(\frac{\mu}{\mu_o}v_z^*\right)\right\} - \rho_o g\left[1 - \frac{\beta(T^* - T_o^*)}{c_t}\right] \qquad (1.1\text{-}19)$$

To make (1.1-19) dimensionless, multiply by

$$\frac{c_v^2 R}{\rho_o N_{Pr}}$$

where N_{Pr} is the Prandtl number, and is defined as

$$N_{Pr} = \frac{\mu_o}{\rho_o \alpha_o} = \frac{\nu_o}{\alpha_o} \tag{1.1-20}$$

where υ_o is the kinematic viscosity (μ_o/ρ_o).

Setting the coefficient of $\partial\rho^*/\partial z^*$ equal to unity gives

$$\frac{c_v^2 R}{\rho_o N_{Pr}} \times \frac{g_o}{c_p' R} = 1 \tag{1.1-21}$$

or

$$c_p' = \frac{R^2 g_o}{\alpha_o \mu_o} \tag{1.1-22}$$

The buoyant force term, F_B, in (1.1-19) becomes

$$F_B = - \frac{R^3 g}{\alpha_o^2 N_{Pr}} \left[1 - \frac{\beta(T^*-T_o^*)}{c_t} \right] \tag{1.1-23}$$

Now the Galileo and Grashof numbers are defined as

$$N_{Ga} = \frac{R^3 g}{\upsilon_o^2} \tag{1.1-24}$$

$$N_{Gr} = \frac{R^3 g \beta \Delta T}{\upsilon_o^2} \tag{1.1-25}$$

where

ΔT = arbitrary reference temperature difference in the fluid.

Using (1.1-24) and (1.1-25) in (1.1-23) gives

$$F_B = - N_{Ga} N_{Pr} + \frac{N_{Gr} N_{Pr} (T^*-T_o^*)}{c_t \Delta T} \tag{1.1-26}$$

Now define

$$c_t = \frac{1}{\Delta T} = \frac{1}{T_1 - T_o} \tag{1.1-27}$$

where

T_1 = arbitrary reference temperature in the fluid, and

T_o = reference temperature at which ρ_o, μ_o, k_o, etc. are evaluated.

Then (1.1-26) becomes

$$F_B = - N_{Ga}N_{Pr} + N_{Gr}N_{Pr}\left(T^*-T_o^*\right) \tag{1.1-28}$$

and the z-component of the momentum equation can finally be written in dimensionless form as

$$\frac{1}{N_{Pr}}\left[v_r^* \frac{\partial v_z^*}{\partial r^*} + \frac{v_\theta^*}{r^*}\frac{\partial v_z^*}{\partial \theta^*} + v_z^* \frac{\partial v_z^*}{\partial z^*}\right] = - \frac{\partial p^*}{\partial z^*}$$

$$+ \frac{1}{r^*}\frac{\partial}{\partial r^*}\left[r^* \frac{\partial}{\partial r^*}\left(\frac{\mu}{\mu_o} v_z^*\right)\right] + \frac{1}{r^{*2}}\frac{\partial^2}{\partial \theta^{*2}}\left(\frac{\mu}{\mu_o} v_z^*\right)$$

$$+ \frac{\partial^2}{\partial z^{*2}}\left(\frac{\mu}{\mu_o} v_z^*\right) - N_{Ga}N_{Pr} + N_{Gr}N_{Pr}\left(T^*-T_o^*\right) \tag{1.1-29}$$

Using the definition of c_t from (1.1-27), equation (1.1-18) can now be solved for c_q to give

$$c_q = \frac{R^2}{k_o(T_1-T_o)} \tag{1.1-30}$$

The use of (1.1-13), (1.1-14), (1.1-20), and (1.1-22) in (1.1-2) results in the dimensionless form of the r-component of the momentum equation

$$\frac{1}{N_{Pr}}\left[v_r^* \frac{\partial v_r^*}{\partial r^*} + \frac{v_\theta^*}{r^*}\frac{\partial v_r^*}{\partial \theta^*} - \frac{v_\theta^{*2}}{r^*} + v_z^* \frac{\partial v_r^*}{\partial z^*}\right]$$

$$= - \frac{\partial p^*}{\partial r^*} + \frac{\partial}{\partial r^*}\left[\frac{1}{r^*}\left(\frac{\mu}{\mu_o}\right)\frac{\partial}{\partial r^*}\left(r^* v_r^*\right)\right] + \frac{1}{r^{*2}}\frac{\partial^2}{\partial \theta^{*2}}\left(\frac{\mu}{\mu_o} v_r^*\right)$$

$$- \frac{2}{r^{*2}}\frac{\partial}{\partial \theta^*}\left(\frac{\mu}{\mu_o} v_\theta^*\right) + \frac{\partial^2}{\partial z^{*2}}\left(\frac{\mu}{\mu_o} v_r^*\right) \tag{1.1-31}$$

Similarly, the dimensionless form of the θ-component of the momentum equation becomes

$$\frac{1}{N_{Pr}}\left[v_r^*\frac{\partial v_\theta^*}{\partial r^*}+\frac{v_\theta}{r^*}\frac{\partial v_\theta^*}{\partial \theta^*}+\frac{v_r^* v_\theta^*}{r^*}+v_z^*\frac{\partial v_\theta^*}{\partial z^*}\right]$$

$$=-\frac{1}{r^*}\frac{\partial p^*}{\partial \theta^*}+\frac{\partial}{\partial r^*}\left[\frac{1}{r^*}\frac{\partial}{\partial r^*}\left(\frac{\mu r^* v_\theta^*}{\mu_o}\right)\right]+\frac{1}{r^{*2}}\frac{\partial^2}{\partial \theta^{*2}}\left(\frac{\mu}{\mu_o}v_\theta^*\right)$$

$$+\frac{2}{r^{*2}}\frac{\partial}{\partial \theta^*}\left(\frac{\mu}{\mu_o}v_r^*\right)+\frac{\partial^2}{\partial z^{*2}}\left(\frac{\mu}{\mu_o}v_\theta^*\right) \qquad (1.1\text{-}32)$$

The dimensionless form of the conservation of mass equation becomes

$$\frac{1}{r^*}\frac{\partial}{\partial r^*}\left(r^* v_r^*\right)+\frac{1}{r^*}\frac{\partial v_\theta^*}{\partial \theta^*}+\frac{\partial v_z^*}{\partial z^*}+\frac{Rc_v W^*}{\rho_o c_w}=0 \qquad (1.1\text{-}33)$$

Setting the coefficient of W* equal to unity gives

$$c_w=\frac{R^2}{\alpha_o \rho_o} \qquad (1.1\text{-}34)$$

The dimensionless form of the energy equation is

$$v_r^*\frac{\partial T^*}{\partial r^*}+\frac{v_\theta^*}{r^*}\frac{\partial T^*}{\partial \theta^*}+v_z^*\frac{\partial T^*}{\partial z^*}=\frac{1}{r^*}\frac{\partial}{\partial r^*}\left[r^*\left(\frac{k}{k_o}\right)\frac{\partial T^*}{\partial r^*}\right]$$

$$+\frac{1}{r^{*2}}\frac{\partial^2}{\partial \theta^{*2}}\left[\left(\frac{k}{k_o}\right)T^*\right]+\frac{\partial^2}{\partial z^{*2}}\left[\left(\frac{k}{k_o}\right)T^*\right]+Q^* \qquad (1.1\text{-}35)$$

The scaling relatinships for conservation of mass, momentum, and energy may now be summarized as follows:

$$r^*=\frac{r}{R} \qquad \theta^*=\theta \qquad z^*=\frac{z}{R}$$

$$v_r^*=\frac{Rv_r}{\alpha_o} \qquad v_\theta^*=\frac{Rv_\theta}{\alpha_o} \qquad v_z^*=\frac{Rv_z}{\alpha_o}$$

$$p^*=\frac{R^2 g_o p}{\alpha_o \mu_o} \qquad T^*=\frac{T}{T_1-T_0} \qquad W^*=\frac{R^2 W}{\alpha_o \rho_o}$$

$$Q^*=\frac{R^2 Q}{k_o(T_1-T_0)} \qquad (1.1\text{-}36)$$

Application of (1.1-36) to the boundary conditions of (1.1-9) gives the dimensionless forms

$$v_r^*(1,\theta^*,z^*) = v_\theta^*(1,\theta^*,z^*) = v_z^*\left(r^*,\theta^*,\frac{Z}{R}\right) = v_z^*(r^*,\theta^*,0) = 0$$

$$\frac{\partial v_r^*(0,\theta^*,z^*)}{\partial r^*} = \frac{\partial v_\theta^*(0,\theta^*,z^*)}{\partial \theta^*} = 0$$

$$p^*\left(r^*,\theta^*,\frac{Z}{R}\right) = 0 \qquad (1.1\text{-}37)$$

Application of (1.1-36) to the boundary condition of (1.1-11) gives

$$\frac{\partial T^*(1,\theta^*,z^*)}{\partial r^*} = -\frac{U_{wall}R}{k}\left[T^*(1,\theta^*,z^*) - T^*\left(\frac{R+\varepsilon}{R},\theta^*,z^*\right)\right]$$

$$\frac{\partial T^*(0,\theta^*,z^*)}{\partial r^*} = \frac{\partial T^*(0,\theta^*,z^*)}{\partial \theta^*} = 0$$

$$T^*\left(0,0,\frac{Z}{2R}\right) = T^*_{bulk}$$

$$\frac{\partial T^*(r^*,\theta^*,0)}{\partial z^*} = -\frac{U_{bott}R}{k}\left[T^*(r^*,\theta^*,0) - T^*\left(r^*,\theta^*,-\frac{\gamma}{R}\right)\right]$$

$$\frac{\partial T^*\left(r^*,\theta^*,\frac{Z}{R}\right)}{\partial z^*} = \frac{-R}{(T_1-T_0)k}\left(\frac{q}{A}\right)_{feed} = -\left(\frac{q}{A}\right)^*_{feed} \qquad (1.1\text{-}38)$$

The first and fourth boundary conditions in (1.1-38) contain a dimensionless group called the Nusselt number. It is defined as

$$N_{Nu} = \frac{UR}{k} \qquad (1.1\text{-}39)$$

and will be of considerable interest later on.

2. Conservation of Electric Charge

In a joule-heated melter, the glass is maintained at a given operating temperature by passing electrical current through it. Metal ions in the molten glass make it a conductor, which possesses a finite, but usually low, resistance. This results in joule-heating or, more commonly, resistance-heating. To optimize the power generation in such a melter and obtain accurate temperature distributions within it, it is necessary to know the voltage and power distributions within the glass.

Consider the volume element in Figure 3. Let J_r be the current flux

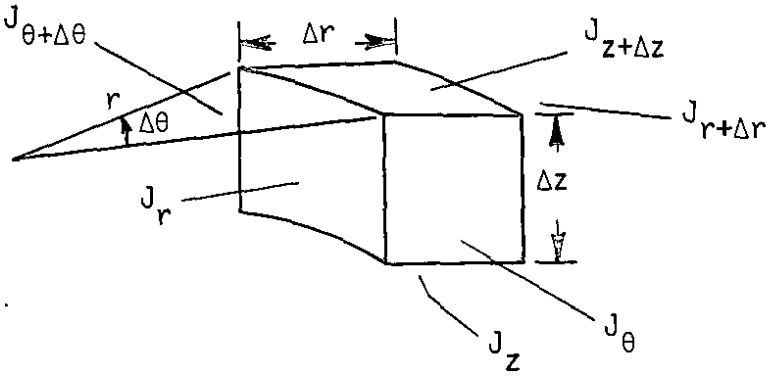

FIGURE 3. Volume Element for Conservation of Electric Charge

entering the element at $r = r$ and $J_{r+\Delta r}$ be the current flux leaving the element at $r = r + \Delta r$. Then a charge balance over the time interval Δt gives

$$\text{charge in} = J_r \, r\Delta\theta\Delta z\Delta t \tag{1.2-1}$$

$$\text{charge out} = J_{r+\Delta r} \, (r+\Delta r) \, \Delta\theta\Delta z\Delta t \tag{1.2-2}$$

where J_r has units of amp/in^2.

Similarly, over the whole volume element one has

$$\left[\rho_e \, (t+\Delta t) - \rho_e(t)\right] \, r \, \Delta r\Delta\theta\Delta z = \left[rJ_r - (r+\Delta r) \, J_{r+\Delta r}\right] \, \Delta\theta\Delta z\Delta t$$
$$+ \left[J_\theta - J_{\theta+\Delta\theta}\right] \Delta r\Delta z\Delta t + \left[J_z - J_{z+\Delta z}\right] r\Delta r\Delta\theta\Delta t$$
$$+ Q_e \, r\Delta\theta\Delta r\Delta z\Delta t \tag{1.2-3}$$

where

$\rho_e(t)$ = total charge density (coul/ft^3) in the volume element at time t

Q_e = charge source or sink term (coul/ft^3-sec).

Dividing by $r\Delta r\Delta\theta\Delta z\Delta t$ gives

$$\frac{\rho_e(t+\Delta t) - \rho_e(t)}{\Delta t} = \frac{r\,J_r - (r+\Delta r)\,J_{r+\Delta r}}{r\Delta r} + \frac{J_\theta - J_{\theta+\Delta\theta}}{r\Delta\theta}$$

$$+ \frac{J_z - J_{z+\Delta z}}{\Delta z} + Q_e \qquad (1.2\text{-}4)$$

Taking $\lim_{\Delta t\to 0}$, $\lim_{\Delta r\to 0}$, $\lim_{\Delta\theta\to 0}$, and $\lim_{\Delta z\to 0}$ gives

$$\frac{\partial\rho_e}{\partial t} = -\frac{1}{r}\frac{\partial}{\partial r}(rJ_r) - \frac{1}{r}\frac{\partial J_\theta}{\partial\theta} - \frac{\partial J_z}{\partial_\delta} + Q_e \qquad (1.2\text{-}5)$$

or more simply

$$\frac{\partial\rho_e}{\partial t} = -\vec{\nabla}\cdot\vec{J} + Q_e \qquad (1.2\text{-}6)$$

Ohm's law can be written as

$$\vec{J} = -\sigma\vec{\nabla}V \qquad (1.2\text{-}7)$$

where

$\vec{J}$ = current flux (amp/in.^{2}),

σ = electrical conductivity $\left(\frac{1}{\Lambda\text{-in.}}\right)$

$= \sigma(T)$

$\vec{\nabla}V$ = voltage gradient (volts/in.)

from which (1.2-6) becomes

$$\frac{\partial\rho_e}{\partial t} = \vec{\nabla}\cdot(\sigma\vec{\nabla}V) + Q_e$$

or

$$\frac{\partial \rho_e}{\partial t} = \frac{1}{r}\frac{\partial}{\partial r}\left[\sigma \frac{\partial}{\partial r}(rV)\right] + \frac{1}{r}\frac{\partial}{\partial \theta}\left[\frac{\sigma}{r}\frac{\partial V}{\partial \theta}\right]$$

$$+ \frac{\partial}{\partial z}\left[\sigma \frac{\partial V}{\partial z}\right] + Q_e \qquad (1.2\text{-}8)$$

Equation (1.2-8) expresses conservation of electrical charge† in three-dimensional cylindrical coordinates. To express this equation in dimensionless form, choose

$$r^* = \frac{r}{R} \qquad \theta^* = \theta \qquad z^* = \frac{z}{R}$$

$$V^* = c_V V \qquad Q_e^* = c_e Q_e \qquad (1.2\text{-}9)$$

Using (1.2-9) in the steady-state form of (1.2-8), i.e., $\frac{\partial \rho_e}{\partial t} = 0$, gives

$$0 = \frac{\sigma_o}{R^2 c_V}\left\{\frac{1}{r^*}\frac{\partial}{\partial r^*}\left[\frac{\sigma}{\sigma_o}\frac{\partial}{\partial r^*}(r^*V^*)\right] + \frac{1}{r^*}\frac{\partial}{\partial \theta^*}\left[\frac{\sigma}{\sigma_o r^*}\frac{\partial V^*}{\partial \theta^*}\right]\right.$$

$$\left. + \frac{\partial}{\partial z^*}\left[\frac{\sigma}{\sigma_o}\frac{\partial V^*}{\partial z^*}\right]\right\} + \frac{Q_e^*}{c_e} \qquad (1.2\text{-}10)$$

where

σ_o = electrical conductivity measured at an arbitrary reference temperature, T_o.

Multiplying (1.2-10) by

$$\frac{R^2 c_V}{\sigma_o} \qquad (1.2\text{-}11)$$

and setting the coefficient of Q_e^* equal to unity gives

$$\frac{R^2 c_V}{\sigma_o c_e} = 1 \qquad (1.2\text{-}11)$$

Choose

$$c_V = \frac{1}{V_o} \qquad (1.2\text{-}12)$$

where

V_o = arbitrary reference potential.

---

† Strictly speaking σ is a function of temperature, T. But $T = T(r,\theta,z)$. Hence σ is not a constant, but must also be differentiated.

Then (1.2-11) gives

$$c_e = \frac{R^2}{\sigma_o V_o} \tag{1.2-13}$$

Thus the steady-state, dimensionless form of the conservation of electrical charge equation is

$$0 = \frac{1}{r^*}\frac{\partial}{\partial r^*}\left[\frac{\sigma}{\sigma_o}\frac{\partial}{\partial r^*}(r^*V^*)\right] + \frac{1}{r^*}\frac{\partial}{\partial \theta^*}\left[\frac{\sigma}{\sigma_o r^*}\frac{\partial V^*}{\partial \theta^*}\right]$$

$$+ \frac{\partial}{\partial z^*}\left[\frac{\sigma}{\sigma_o}\frac{\partial V^*}{\partial z^*}\right] + Q_e^* \tag{1.2-13}$$

where

$$r^* = \frac{r}{R} \qquad \theta^* = \theta \qquad z^* = \frac{z}{R}$$

$$V^* = \frac{V}{V_o} \qquad Q_e^* = \frac{R^2 Q_e}{\sigma_o V_o} \tag{1.2-14}$$

Applicable boundary conditions for (1.2-13) are: (1) that no current leaves the system

$$\left.\frac{\partial V}{\partial r}\right|_{r=R} = \left.\frac{\partial V}{\partial \theta}\right|_{r=R} = \left.\frac{\partial V}{\partial z}\right|_{z=0} = \left.\frac{\partial V}{\partial z}\right|_{z=Z} = 0 \tag{1.2-15}$$

and (2) that the system be symmetric with respect to r and θ at the center

$$\left.\frac{\partial V}{\partial \theta}\right|_{r=0} = \left.\frac{\partial V}{\partial r}\right|_{r=0} = 0 \tag{1.2-16}$$

Using (1.2-14) in the boundary conditions gives the dimensionless forms

$$\left.\frac{\partial V^*}{\partial r^*}\right|_{r^*=1} = \left.\frac{\partial V^*}{\partial \theta^*}\right|_{r^*=1} = \left.\frac{\partial V^*}{\partial z^*}\right|_{z^*=0} = \left.\frac{\partial V^*}{\partial z^*}\right|_{z^*=\frac{Z}{R}} = 0 \tag{1.2-17}$$

and

$$\left.\frac{\partial V^*}{\partial \theta^*}\right|_{r^*=0} = \left.\frac{\partial V^*}{\partial r^*}\right|_{r^*=0} = 0 \tag{1.2-18}$$

Note that the boundary conditions are automatically satisfied in either the melter or the model by simply having an electrically insulated container.

3. Electrode Current

The charge source/sink term Q_e can be used to determine the current flow, I, through an electrode as follows. Let

$$I = \iiint Q_e \, r dr d\theta dz \tag{1.3-1}$$

where the integration is performed over the electrode volume. If the dimensionless electrode current is

$$I^* = C_I I \tag{1.3-2}$$

then the use of (1.2-14) in (1.3-1) gives

$$\frac{I^*}{C_I} = \frac{\sigma_o V_o}{R^2} \iiint Q_e^* \, R^3 r^* dr^* d\theta^* dz^*$$

or

$$C_I = \frac{1}{\sigma_o V_o R} \tag{1.3-3}$$

Hence,

$$I^* = \frac{I}{\sigma_o V_o R} \tag{1.3-4}$$

which provides a means of predicting electrode current in the melter based upon that measured in the model.

4. Power Density

The power density, P (watts/ft^3), may be defined as

$$P = - \vec{\nabla} V \cdot \vec{J} \tag{1.4-1}$$

where

$\vec{\nabla} V$ = voltage gradient (volts/in)

$\vec{J}$ = current flux (amps/in^2)

Using Ohm's law, (1.4-1) becomes

$$P = -\vec{\nabla}V \cdot (-\sigma\vec{\nabla}V) \tag{1.4-2}$$

In cylindrical coordinates, (1.4-2) becomes

$$P = \frac{1}{r}\frac{\partial}{\partial r}(rV)\left[\frac{\sigma}{r}\frac{\partial}{\partial r}(rV)\right] + \frac{1}{r}\frac{\partial V}{\partial \theta}\left[\frac{\sigma}{r}\frac{\partial V}{\partial \theta}\right] + \frac{\partial V}{\partial z}\left[\sigma\frac{\partial V}{\partial z}\right]$$

$$= \frac{\sigma}{r^2}\left[\frac{\partial (rV)}{\partial r}\right]^2 + \frac{\sigma}{r^2}\left[\frac{\partial V}{\partial \theta}\right]^2 + \sigma\left[\frac{\partial V}{\partial z}\right]^2 \tag{1.4-3}$$

This equation provides the energy input rate, Q, in the conservation of energy equation (1.1-10) via the conversion

$$Q\ [\text{Btu/ft}^3\text{-sec}] = 9.478 \times 10^{-4}\ P\ [\text{watts/ft}^3] \tag{1.4-4}$$

Using (1.2-14) in (1.4-3) and defining the dimensionless power density as

$$P^* = c_{pow} P \tag{1.4-5}$$

gives

$$\frac{P^*}{c_{pow}} = \frac{\sigma_o V_o^2}{R^2}\left\{\frac{1}{r^{*2}}\left(\frac{\sigma}{\sigma_o}\right)\left[\frac{\partial}{\partial r^*}(r^*V^*)\right]^2 + \left(\frac{\sigma}{\sigma_o}\right)\frac{1}{r^{*2}}\left[\frac{\partial V^*}{\partial \theta^*}\right]^2 + \left(\frac{\sigma}{\sigma_o}\right)\left[\frac{\partial V^*}{\partial z^*}\right]^2\right\} \tag{1.4-6}$$

Setting

$$c_{pow} = \frac{R^2}{\sigma_o V_o^2} \tag{1.4-7}$$

reduces (1.4-6) to dimensionless form†, and gives

$$P^* = \frac{R^2 P}{\sigma_o V_o^2} \tag{1.4-8}$$

which provides a means of predicting local power density in a melter from power density in a model.

---

† (1.4-6) indicates that the power density is proportional to the square of the voltage gradient.

5. Total Power

The total power generated in an arbitrary volume can be obtained by integrating (1.4-1) over the volume to get

$$P_{tot} = -\iiint \nabla V \cdot \vec{J}\, r dr d\theta dz \qquad (1.5\text{-}1)$$

Using (1.4-2) and (1.4-3) gives

$$P_{tot} = \iiint \frac{\sigma}{r^2}\left[\frac{\partial}{\partial r}(rV)\right]^2 r dr d\theta dz + \iiint \frac{\sigma}{r^2}\left[\frac{\partial V}{\partial \theta}\right]^2 r dr d\theta dz$$

$$+\iiint \sigma\left[\frac{\partial V}{\partial z}\right]^2 r dr d\theta dz \qquad (1.5\text{-}2)$$

Again using (1.2-14) and defining

$$P^*_{tot} = c_{tot}\, P_{tot}, \qquad (1.5\text{-}3)$$

equation (1.5-2) becomes

$$\frac{P^*}{c_{tot}} = \sigma_o V_o^2 R\left\{\iiint\left(\frac{\sigma}{\sigma_o}\right)\frac{1}{r^{*2}}\left[\frac{\partial}{\partial r^*}(r^*V^*)\right]^2 r^* dr^* d\theta^* dz^*\right.$$

$$+\iiint\left(\frac{\sigma}{\sigma_o}\right)\frac{1}{r^{*2}}\left[\frac{\partial V^*}{\partial \theta^*}\right]^2 r^* dr^* d\theta^* dz^*$$

$$\left.+\iiint\left(\frac{\sigma}{\sigma_o}\right)\left[\frac{\partial V^*}{\partial z^*}\right]^2 r^* dr^* d\theta^* dz^*\right\} \qquad (1.5\text{-}4)$$

Setting

$$c_{tot} = \frac{1}{R\sigma_o V_o^2} \qquad (1.5\text{-}5)$$

makes (1.5-4) dimensionless and gives

$$P^*_{tot} = \frac{P_{tot}}{R\sigma_o V_o^2} \qquad (1.5\text{-}6)$$

Equation (1.5-6) can be used to predict total power consumption in the melter based upon total power consumption in the model.

6. Current Flux

The current flux in a joule-heated melter is of particular interest on electrode surfaces since its magnitude there is thought to be related to electrode lifetime.

Let $\hat{n}$ be a unit vector normal to an arbitrary surface, S (Figure 4). Using

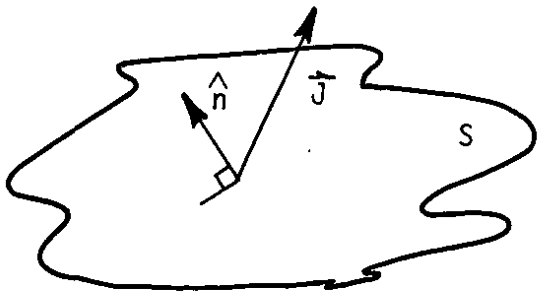

FIGURE 4. Current Flux Impinging on an Arbitrary Surface

Ohm's law, the component of the current flux, $\vec{J}$, normal to S is

$$\vec{J}\cdot\hat{n} = -\sigma\vec{\nabla}V\cdot\hat{n}$$

or

$$J_n = -\frac{\sigma}{r}\frac{\partial}{\partial r}(rV)\,n_r - \frac{\sigma}{r}\frac{\partial V}{\partial\theta}\,n_\theta - \sigma\frac{\partial V}{\partial z}\,n_z \qquad (1.6\text{-}1)$$

where

J_n = magnitude of the current flux in the direction of $\hat{n}$

n_r, n_θ, n_z = components of the unit vector $\hat{n}$

Using (1.2-14) in (1.6-1) and defining

$$J_n^* = c_J\,J_n$$

$$n_r^* = \frac{n_r}{|\hat{n}|},\quad n_\theta^* = \frac{n_\theta}{|\hat{n}|},\quad n_z^* = \frac{n_z}{|\hat{n}|} \qquad (1.6\text{-}2)$$

gives

$$\frac{J_n^*}{c_J} = -\frac{\sigma_o V_o}{R}\left\{\left(\frac{\sigma}{\sigma_o}\right)\frac{1}{r^*}\frac{\partial(r^*V^*)}{\partial r^*}\,n_r^* + \left(\frac{\sigma}{\sigma_o}\right)\frac{1}{r^*}\frac{\partial V^*}{\partial\theta^*}\,n_\theta^* + \left(\frac{\sigma}{\sigma_o}\right)\frac{\partial V^*}{\partial z^*}\,n_z^*\right\} \qquad (1.6\text{-}3)$$

which becomes dimensionless if one sets

$$c_J = \frac{R}{\sigma_o V_o} \tag{1.6-4}$$

This gives

$$J_n^* = \frac{RJ_n}{\sigma_o V_o} \tag{1.6-5}$$

Since current flux is not a directly measurable quantity, it is more convenient for data analysis to cast (1.6-5) in terms of voltage gradients.

If $\hat{n}$ is selected as a unit vector in the r-direction, then (1.6-1) and (1.6-5) give

$$J_r^* = \frac{R}{\sigma_o V_o}\left[-\frac{\sigma}{r}\frac{\sigma(rV)}{\partial r}\right] \tag{1.6-6}$$

or approximately

$$J_r^* \simeq -\frac{R}{V_o}\left(\frac{\bar{\sigma}}{\sigma_o}\right)\left[\frac{r_2V_2 - r_1V_1}{r_2 - r_1}\right] \tag{1.6-7}$$

where

$$\bar{\sigma} = \sigma(\bar{T}) \tag{1.6-8}$$

and $\bar{T}$ is the average temperature in the volume element under consideration.

Similarly, for current flux in the θ and z directions, one has

$$J_\theta^* = \frac{R}{\sigma_o V_o}\left[-\frac{\sigma}{r}\frac{\partial V}{\partial \theta}\right]$$

$$\simeq -\frac{R}{rV_o}\left(\frac{\bar{\sigma}}{\sigma_o}\right)\left[\frac{V_2 - V_1}{\theta_2 - \theta_1}\right] \tag{1.6-9}$$

and

$$J_z^* = \frac{R}{\sigma_o V_o}\left[-\sigma\frac{\partial V}{\partial z}\right]$$

$$\simeq -\frac{R}{V_o}\left(\frac{\sigma}{\sigma_o}\right)\left[\frac{V_2 - V_1}{z_2 - z_1}\right] \tag{1.6-10}$$

7. Electrical Resistance

By definition, the electrical resistance, R(ohms), between two points ℓ (inches) apart is given by

$$R = \frac{\rho_{el}\,\ell}{A} \tag{1.7-1}$$

where

ρ_{el} = resistivity of the medium (ohm-inches)

= reciprocal of the conductivity, σ

A = cross-sectional area through which the current passes ($in.^2$).

A characteristic of most glasses is that the resistivity falls approximately exponentially with increasing temperature. Thus, the temperature distribution in a glass melter strongly influences its overall resistance.

Choose

$$\ell^* = \frac{\ell}{\ell_o},\quad A^* = \frac{A}{A_o} \tag{1.7-2}$$

where

ℓ_o = arbitrary reference length in the melter

A_o = arbitrary reference area in a plane perpendicular to ℓ_o

Then let

$$R^* = c_R R \tag{1.7-3}$$

and (1.7-1) becomes

$$\frac{R^*}{c_R} = \frac{\rho_{el}\,\ell^*}{\rho_{elo}\,A^*} \times \frac{\ell_o\,\rho_{elo}}{A_o} \tag{1.7-4}$$

where

ρ_{elo} = resistivity of the glass measured at an arbitrary reference temperature, T_o.

Setting

$$c_R = \frac{A_o}{\rho_{elo}\, \ell_o} \tag{1.7-5}$$

makes (1.7-4) dimensionless, and from (1.7-3)

$$R^* = \frac{A_o R}{\rho_{elo}\, \ell_o} \tag{1.7-6}$$

Equation (1.7-6) can be used to predict the resistance of the melter based upon the resistance of the model.

II. Similarity Requirements for Modeling

If a model can be designed such that the dimensionless numbers (ratios) for the model are equal to those in the glass melter, then it follows that the model will satisfy the same conservation equations that apply to the melter. This condition is known as physical similarity, and such a model is called a physical model. More explicitly, it means that dependent variables such as pressure, temperature, velocity, voltage, etc. that are measured in the model will have the same dimensionless values in the melter.

Since in practice, it is very difficult to match every dimensionless number in the two systems, consider the following simplifications. If one allows no mass input or output in the model, then

$$W^* = 0 \tag{2.1-1}$$

and the conservation of mass equation (1.1-33) can be matched by simply using (1.1-36).

Inspection of the z-component of the momentum equation (1.1-29) indicates that in addition to matching (1.1-36), one must also match $\mu/\mu o$, N_{Pr}, $N_{Ga}N_{Pr}$, and $N_{Gr}N_{Pr}$. The glass, however, has a large Prandtl number and moves extremely slowly and thereby indicates that the left hand side of (1.1-29) is small. Hence, it suffices in the model to choose a model fluid which also has a large Prandtl number.

The gravitational force on the glass exceeds the buoyant force by several orders of magnitude. Thus, the pressure, p, at any point, z, below the surface, z = Z, can be closely approximated by

$$p = -\rho_o (z - Z)\, g/g_o \tag{2.1-2}$$

and

$$-g_o \frac{\partial p}{\partial z} = \rho_o g \qquad (2.1\text{-}3)$$

which cancels the term $-\rho_o g$ in (1.1-8) and deletes $N_{Ga}\, N_{Pr}$ from (1.1-29). If, however, there is mass throughput, i.e. $W^* \neq 0$, then (2.1-2) is not an accurate representation of p, and it becomes necessary to match the product $N_{Ga}\, N_{Pr}$.

It is also necessary to match the product $N_{Gr}\, N_{Pr}$, which represents the buoyant force in the glass. This product is known as the Rayleigh number,

$$N_{Ra} = N_{Gr}\, N_{Pr} = \frac{R^3 g \beta \Delta T}{\nu_o \alpha_o} \qquad (2.1\text{-}4)$$

and is of primary interest in modeling a glass melter.† The viscosity ratio, μ/μ_o, appears only in the shear force terms which are negligibly small compared to the buoyant force.

However, in the r- and θ-components of the momentum equations [(1.1-31) and (1.1-32)], no buoyant force terms appear and by (2.1-2)

$$\frac{\partial p^*}{\partial r^*} = \frac{\partial p^*}{\partial \theta^*} = 0 \qquad (2.1\text{-}5)$$

Thus, to accurately model v_r^* and v_θ^*, it is important that one match N_{Pr} and μ/μ_o. In practice, it is difficult to match both the Prandtl number and the Rayleigh number in a model. The usual choice is to match the Rayleigh number and simply require that the Prandtl number be large. This results in good agreement of v_z^* and an accurate ΔT prediction†† for the melter indicated by model data. However, the agreement between v_r^* and v_θ^* is necessarily somewhat poorer.

---

† Note that (1.1-29) may be divided through by the Prandtl number, in which case the modeling constraints are a large Prandtl number and matching of the Galileo and Grashof numbers. However, the choice of the model fluid is a little easier using the method described in the text.

†† Since the definition of ΔT is arbitrary [cf. (1.1-27)], it may conveniently be chosen as the maximum temperature difference in the model and the melter. If the Rayleigh numbers are matched in the two systems, then the model can be used to predict the maximum ΔT in the melter.

Inspection of the energy equation (1.1-35) indicates that the thermal conductivity ratio, k/k_o, should be matched in both systems. Most of the energy transfer is by convection. Nevertheless, the ratio, k/k_o, is easily matched and should probably be done. It is especially important that the energy input rate Q^* be matched in the two systems since it directly affects the buoyant force through the temperature T††.

Application of the boundary conditions of (1.1-38) suggests two mechanisms for matching the slope of the temperature profile ($\partial T^*/\partial r^*$) at the inner wall of the model. If the Nusselt number is matched in the model and the melter, and the temperature on the outside of the tank is assumed to be the same for both systems, then the dimensionless temperature on the inside of the tank wall can be modeled absolutely.

Alternatively, $\partial T^*/\partial r^*$ can be matched by simply equating the product of the Nusselt number and the dimensionless temperature drop across the wall in both systems. This enables one to use the model to simulate the effect of different wall compositions in the melter by varying the temperature drop across the wall in the model.††† However, the absolute wall temperature on the inside of the melter can no longer be scaled from model data, but by matching Rayleigh numbers in the two systems, the maximum ΔT in the melter can still be predicted by the model.

The conservation of electrical charge equation can be matched using (1.2-14) and requiring that the conductivity ratio, σ/σ_o, match in both systems. The boundary conditions [(1.2-17) and (1.2-18)] require only that the model have nonconducting walls and be symmetrical about the z-axis.

No additional requirements are placed on the model to achieve similarity of electrode current, power density, total power, current flux, and electrical resistance.

To summarize, it is of primary importance that the model and the melter have:

1) geometric similarity, i.e., all dimensions and lengths must have the same values of r^*, θ^*, and z^*,

2) the same Rayleigh numbers and a large Prandtl number to match convective circulation patterns,

---

†† See footnote †† on previous page.

††† This implies changing the bulk operating temperature in the model.

3) the same heat transfer boundary conditions, i.e., $\partial T^*/\partial r^*$ and $\partial T^*/\partial z^*$, to match temperature profiles,

4) the same power density distribution, P^* (or Q^*), to match convective circulation patterns, and

5) the same electrical conductivity ratio, $\sigma/\sigma o$, to match voltage profiles.

III. Characteristics of the Glass Melter

It is important to reiterate at this point that the purpose of the current modeling program is to better understand the operation of the proposed glass melter and to optimize its design and operation. Thus, it is necessary to characterize the conceptual melter design to provide the basis for design of the model.

The melter is a cylindrical vessel (Figure 5) 64 in. OD and 95 in. high. It has a 48 in. ID with a melt depth of approximately 36 in. The glass is contained by 8 in. of Monofrax† K3 refractory brick below the meltline, and above the meltline, 8 in. of Mullfrax† 202 is used. Outside the brick is a 1 in. thick stainless steel, water-cooled jacket.

Glass frit and calcined waste are fed to the melter through the top. This mixture is brought to 1150°C which melts the frit and provides some mixing of the frit and waste. Then the molten glass is partially withdrawn by tilting the melter to permit pouring through the slanted riser into a stainless steel canister.

Power to the melter is provided by four, cylindrical, air-cooled electrodes made of Inconel†† 690. The electrodes are spaced 90° apart circumferentially at a distance of 17 in. from the center of the tank. They extend 30 in. below the meltline. Each pair of diametrically opposite electrodes is connected to a source of alternating current, shifted 90° in phase from the other pair. Passage of electrical current through the molten glass heats the glass by joule-heating. The design capacity is 2.2 tons of glass per day.

When the melter is active, a cold cap forms on the top due to the buildup of frit and calcined waste, resulting in an estimated glass surface temperature of 800°C. When the melter is

† Trademark of the Carborundum Company.

†† Alloy of the International Nickel Company.

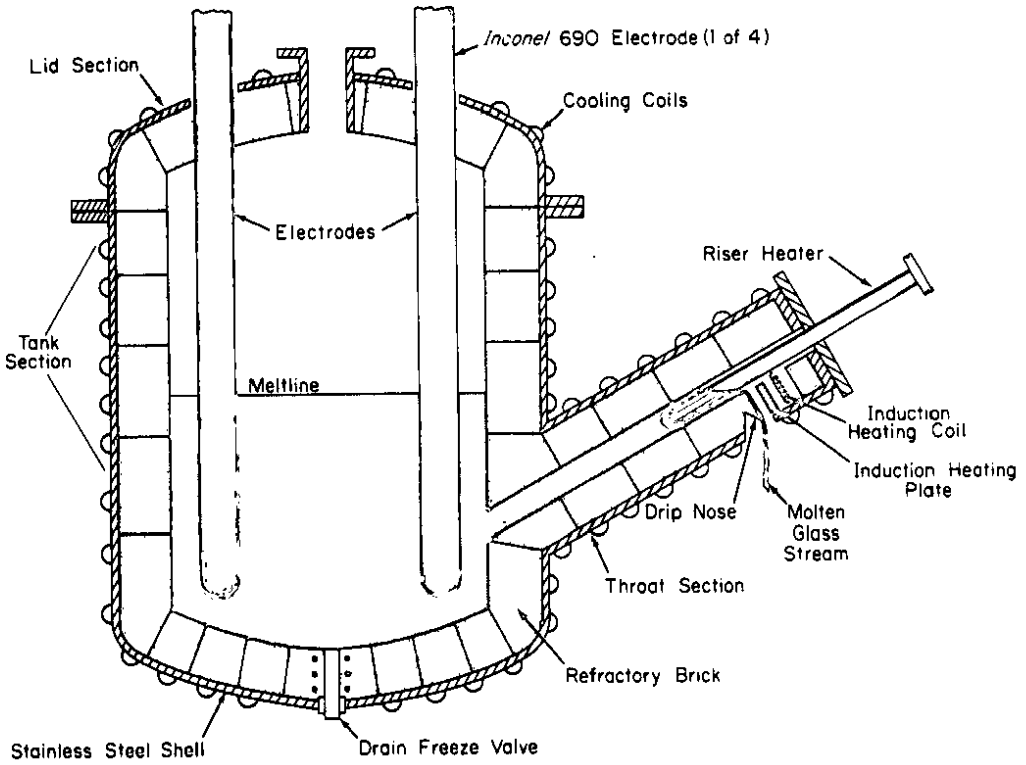

FIGURE 5. Cylindrical Melter Design

idle (no incoming feed) the cold cap melts away, and the glass surface temperature rises to approximately 1000°C. It is assumed to be held there by silicon carbide heating elements in the top portion of the melter.

For modeling purposes, consider only the melt chamber below the melt line. Then the melter can be approximated as in Figure 6. Note that the bottom has been flattened and the slanted riser has been omitted. Pertinent heat transfer data are given in Table 1.

The frit-waste mixture in the melter is known as Frit 21 +27.5 wt % composite sludge (Tables 2 and 3). Typical physical properties of the resulting glass are given in Table 4.

IV. Characteristics of the Physical Model

Several articles have appeared in the literature regarding physical modeling of electrically heated glass melters.[3-9] The most widely used system is a geometrically-scaled plexiglass tank with a modeling fluid composed of glycerine and 5 to 10 wt % LiCl. Stanek[10] has tabulated the physical and electrical properties of this fluid in a convenient form for model design.

1. Design

Assuming that the melter operates with a maximum bulk temperature of 1150°C and a wall temperature of 1050°C and arbitrarily picking T_o = 1100°C, gives a Rayleigh number (cf. Table 4) of

$$N_{Ra} = \frac{R^3 \beta \Delta T g}{\nu_o \alpha_o} = 5.51 \times 10^6 \qquad (3.1\text{-}1)$$

If the scale, S, of the model is chosen to be

$$S = \frac{R_m}{R_e} = \frac{1}{2} \qquad (4.1\text{-}2)$$

where the subscripts, m and e, denote the model and the melter, respectively, then matching Rayleigh numbers in the two systems requires

$$\left.\frac{R^3 \beta \Delta T g}{\nu_o \alpha_o}\right|_m = 5.51 \times 10^6 \qquad (4.1\text{-}3)$$

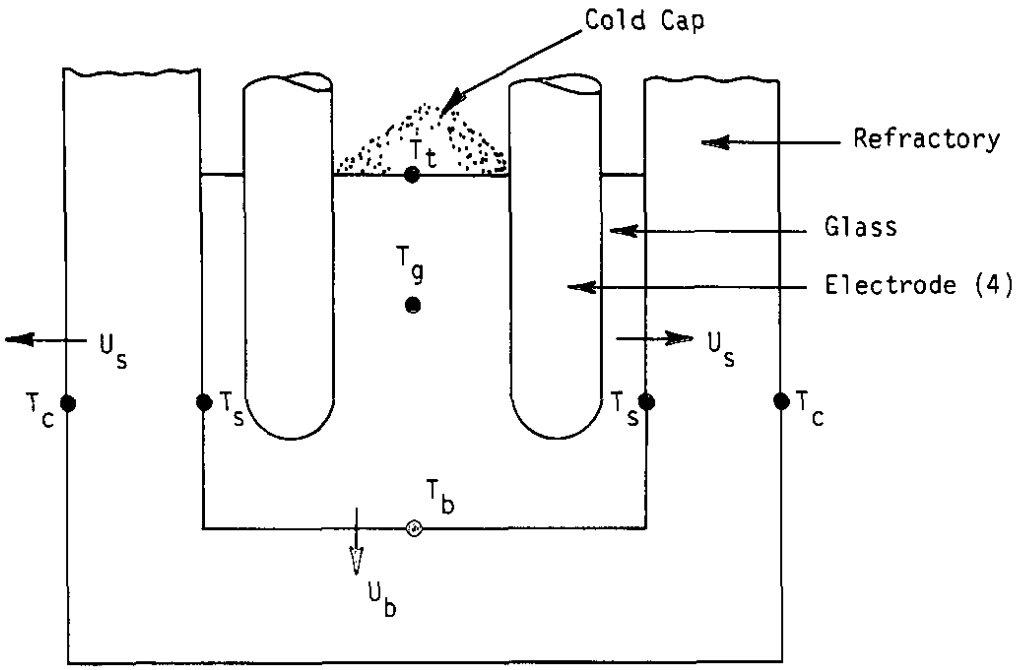

Vertical Section

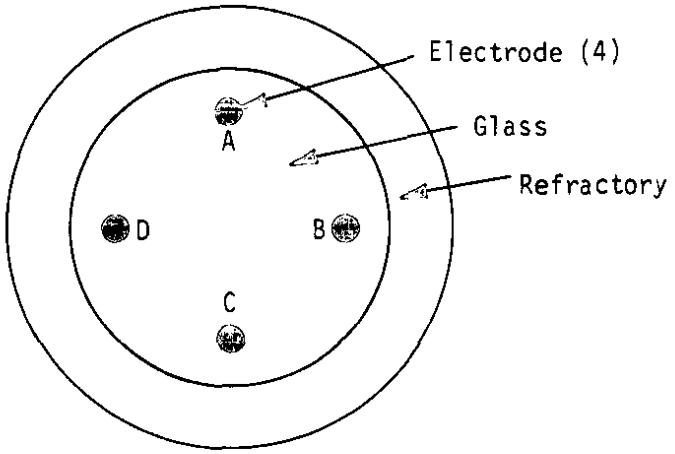

Top View

FIGURE 6. Vertical and Top View of Melter

TABLE 1

Heat Transfer Characteristics of the Glass Melter†

	T, °C	U, pcu/hr-ft²-°C	A, ft²	N_{Nu}	$\frac{\partial T^*}{\partial R^*}$	$\frac{\partial T^*}{\partial Z^*}$
Top - Idle	1000	--	12.6	--	--	-36.0
- Active	800	--	12.6	--	--	-83.9††
Sides	1050	3.62	37.7	3.20	-33.6	--
Bottom	1050	3.13	12.6	2.77	--	27.7

† Glass temperature (T_g): 1150°C.
Coolant temperature (T_c): 50°C.

†† Estimated from the heat required to melt 2.2 tons/day.

TABLE 2

Composition of Glass Frit 21

Component	*Wt %*
SiO_2	52.5
Na_2O	18.5
TiO_2	10.0
B_2O_3	10.0
CaO	5.0
Li_2O	4.0

TABLE 3

Composition of Simulated Composite Sludge

Component	*Wt %*
Fe_2O_3	31.6
Al_2O_3	46.4
MnO_2	10.3
U_3O_8	6.1
CaO	3.3
NiO	2.3

Using Stanek's tabulation of glycerine +LiCl properties, a glycerine +10 wt % LiCl solution was selected.† Properties of this fluid are given in Table 5. Choosing T_o = 30°C for the model, and solving (4.1-3) for ΔT gives

$$\Delta T_m = 8.5°C = 15.3°F \qquad (4.1\text{-}4)$$

from which one concludes that an 8.5°C temperature difference in the model should correspond to a temperature difference of approximately 100°C in the melter.

Comparing the data for the glass in the temperature range 1050° to 1150°C (Table 4) and that of the model fluid in the range of 30 to 40°C (Table 5) against the similarity requirements of Section II confirms that both systems have a large Prandtl number and that the ratios, k/ko and $\mu/\mu o$, are reasonably well matched. Also the ratio σ/σ_o matches for both systems as seen in the tables.

To match the heat transfer boundary conditions, $\partial T^*/\partial r^*$ and $\partial T^*/\partial z^*$, one first attempts to match Nusselt numbers for the two systems. However, for a cylindrical model constructed of Plexiglas® backed by water cooling, this leads to an unreasonably large wall thickness. The alternative is to match the boundary conditions by matching the product of the Nusselt number and the temperature difference across the wall. This alternative was chosen and the wall thickness of the model was selected primarily by structural requirements.

Physical similarity between the power distribution in the melter and the model first of all requires geometrical similarity. For a one-half-scale model, this requires that all electrode dimensions be one-half of the melter electrode dimensions, and that the model electrodes be placed at the same values of r*, θ*, and z* in the model tank as in the melter.

To obtain the desired 90° phase separation in the AC potential between electrode pairs AC and BD (Figure 6), consider a conventional three-phase, four wire, power transmission system connected to the model as shown in Figure 7. Let the potential between each phase and the neutral (usually grounded) be V_A, V_B,

---

† This solution was prepared by bringing the glycerine to 180°C, adding the LiCl, holding the fluid at 180°C for 60 minutes, and then allowing it to cool slowly to ambient temperature.

® Trademark of Rohm and Haas Company.

TABLE 4.

Physical Properties of Frit 21 + 27.5 wt % Composite Sludge

Temperature, °C	1000	1100	1150	1200
Thermal Conductivity k, pcu/hr-ft-°C	1.73	2.26	2.55	2.81
Specific Heat c_p, Pcu/lb-°C	.328	.332	.333	.334
Density ρ, lbm/ft^3	148.8	147.7	147.1	146.5
Volumetric Coefficient of Expansion β, 1/°C	7.62×10^{-5}	7.62×10^{-5}	7.62×10^{-5}	7.62×10^{-5}
Absolute Viscosity μ, poise	154	61.0	43.0	32.0
Electrical Resistivity, ρ_{el} (ohm-cm)	6.0	2.5	1.5	0.9
Kinematic Viscosity = μ/ρ, Stokes	64.6	25.8	18.3	13.6
Thermal Diffusivity $\alpha = k/\rho c_p$, ft^2/hr	.0354	.0461	.0521	.0574
Prandtl Number N_{Pr}	7071	2167	1361	918
μ(T)/μ(1100°C)	2.53	1.00	.705	.525
k(T)/k(1100°C)	.765	1.00	1.13	1.24
σ(T)/ (1100°C) = ρ_{el}(1100°C)/ρ_{el}(T)	.417	1.00	1.67	2.78

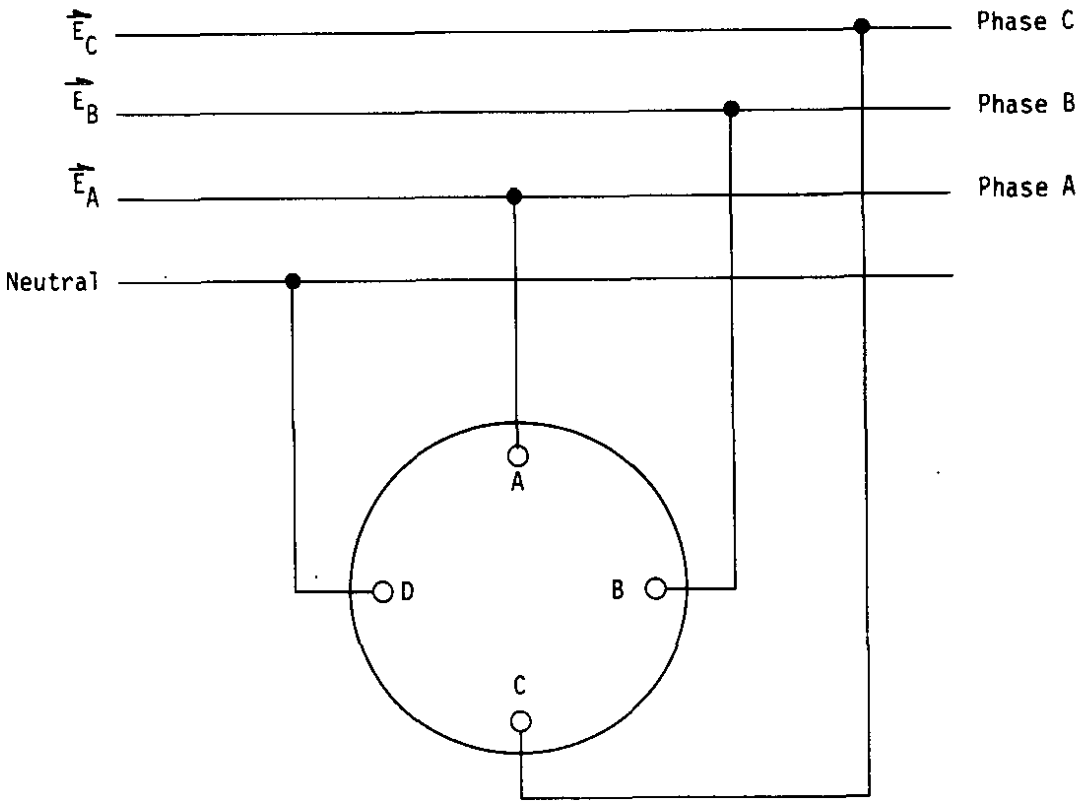

FIGURE 7. Simplified Power Transmission System Connected to the Model

TABLE 5

Physical Properties of the Model Fluid

Temperature T, °C	20	30	40	50	60
*Thermal Conductivity k, pcu/hr-ft-°C	.171	.168	.165	.163	.160
*Specific Heat c_p, pcu/lb-°C	.564	.576	.588	.600	.614
†Density, ρ, lbm/ft^3	81.4	81.0	80.7	80.3	79.9
*Volumetric Coefficient of Expansion, β, 1/°C	4.62×10^{-4}	4.62×10^{-4}	4.62×10^{-4}	4.62×10^{-4}	4.62×10^{-4}
¶Absolute Viscosity, μ, poise	100	27.6	6.80	2.02	1.49
*Electrical Resistivity ρ_{el}, ohm-cm	8600	4600	2600	1110	600
Kinematic Viscosity, $\nu = \mu/\rho$, Stokes	76.7	21.3	5.26	1.57	1.16
Thermal Diffusivity, $\alpha = k/\rho c_p$, ft^2/hr	.00372	.00360	.00348	.00338	.00326
Prandtl Number, N_{Pr}	79900	22900	5857	1800	1379
$\mu(T)/\mu(30°C)$	3.62	1.00	.246	.0732	.0540
$k(T)/k(30°C)$	1.02	1.00	.982	.970	.952
$\sigma(T)/\sigma(30°C) = \rho_{el}(30°C)/\rho_{el}(T)$	.535	1.00	1.77	4.14	7.67

* Properties assumed to be those of pure glycerin.

† Data courtesy of J. R. Wiley, Savannah River Laboratory.

¶ Data courtesy of J. M. Plodinec, Savannah River Laboratory.

and V_C, respectively. These three potentials are generated 120° out-of-phase with one another such that

$$V_A = E_o \sin \theta$$

$$V_B = E_o \sin (\theta + 120°)$$

$$V_c = E_o \sin (\theta + 240°) \qquad (4.1\text{-}5)$$

where the angle, θ, is related to the frequency, f, of the AC signal by

$$\theta = 360° \times f \times t \qquad (4.1\text{-}6)$$

where t = time, sec

E_o = magnitude (maximum value) of the potential between each phase and neutral.

If the three phases are considered as vectors in Cartesian coordinates (Figure 8), then one can write

$$\vec{E}_A = E_o \cos 0° \hat{i} + E_o \sin 0° \hat{j}$$

$$\vec{E}_B = E_o \cos 120° \hat{i} + E_o \sin 120° \hat{j}$$

$$\vec{E}_c = E_o \cos 240° \hat{i} + E_o \sin 240° \hat{j}$$

where $\hat{i}$ = unit vector in x-direction

$\hat{j}$ = unit vector in y-direction (4.1-7)

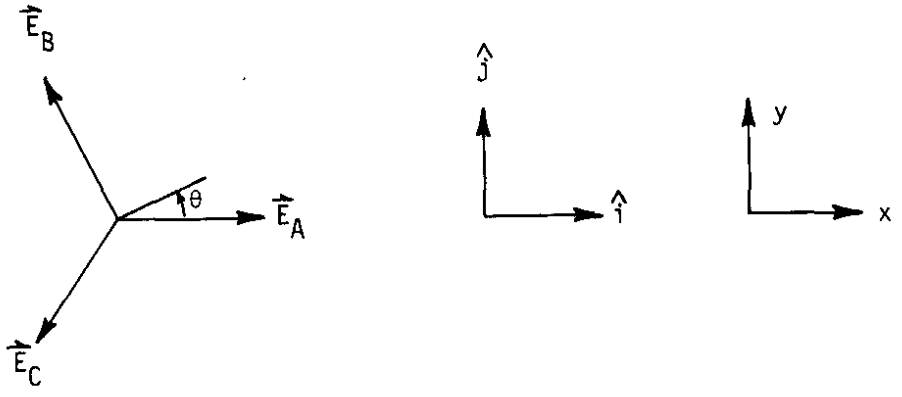

FIGURE 8. Three Phases Represented as Vectors

The vector potential between electrodes A and C is

$$\vec{E}_A - \vec{E}_C = E_o [\cos 0° - \cos 240°] \hat{i}$$

$$+ E_o [\sin 0° - \sin 40°] \hat{j}$$

$$= \frac{3}{2} E_o \hat{i} + \frac{\sqrt{3}}{2} E_o \hat{j} \qquad (4.1\text{-}8)$$

with magnitude

$$\left| \vec{E}_A - \vec{E}_C \right| = \left\{ \left(\frac{3}{2} E_o \right)^2 + \left(\frac{\sqrt{3}}{2} E_o \right)^2 \right\}^{1/2}$$

$$= \sqrt{3} \; E_o \qquad (4.1\text{-}9)$$

The phase angle, θ_{AC}, of $\vec{E}_A - \vec{E}_C$ can be found by considering a unit vector $\hat{\eta}$ in the direction of $\vec{E}_A - \vec{E}_C$, i.e.,

$$\hat{\eta} = \frac{\vec{E}_A - \vec{E}_C}{\left| \vec{E}_A - E_C \right|} = \frac{\sqrt{3}}{2} \hat{i} + 1/2 \; \hat{j} \qquad (4.1\text{-}10)$$

Setting

$$\cos \theta_{AC} = \frac{\sqrt{3}}{2}$$

or

$$\sin \theta_{AC} = 1/2 \qquad (4.1\text{-}11)$$

gives the phase angle

$$\theta_{AC} = 30° \qquad (4.1\text{-}12)$$

Thus, the potential between electrodes A and C is

$$V_{AC} = \sqrt{3} \, E_o \sin (\theta + 30°) \qquad (4.1\text{-}13)$$

and is 90° out of phase with the potential V_B applied between electrodes B and D. A transformer can be used to stepdown V_{AC} to match V_B so that both electrode pairs fire equally.

2. Construction

The model was constructed using a one-half scale, cylindrical, Plexiglas® tank (Figures 9 and 10), and placed inside a larger rectangular tank which provides containment for the cooling water. Two independently controlled cooling jackets were used, one for the sides and bottom, and a second for the top. The model fluid was glycerine +10 wt % LiCl (Table 5).

Four cylindrical electrodes were used, each 3 in. OD × 15 in. long, and mounted on threaded support rods which permitted adjusting their elevation. Copper was chosen as the electrode material, although other materials were tried. There is a reaction between glycerine and metals above hydrogen in the electrochemical series of the form

$$RO\text{-}H + M \rightarrow ROM + 1/2\ H \uparrow \qquad (4.2\text{-}1)$$

where R is any alkyl or substituted alkyl group and M is a metal. This reaction was unapparent (no gas evolution) until an AC potential was applied to the electrodes. It then proceeded vigorously with gas evolution on electrode surfaces and rapid discoloration of the model fluid. It was also found helpful to buff the electrodes (or clean with dilute HNO_3) before inserting them into the model fluid to remove Cu_2O which otherwise tended to slough off and cloud the model fluid.

Small Plexiglas® tubes 7/16 in. OD × 3/16 in. ID were inserted through the top cooling jacket at 1 in. intervals from the center of the tank to the wall and in increments of 45° around the circumference of the tank. Through these tubes, called signal sleeves, 1/16 in. OD copper-constantan thermocouples with stainless steel sheaths were inserted into the model fluid and used to map temperature profiles. It was necessary to insert the thermocouples in heat-shrinkable tubing to prevent the chemical reaction described above.

Thermocouples were attached to fifteen points on the outside of the cylindrical tank to aid in determination of heat transfer boundary conditions. The inlet and exit water temperature to both cooling jackets was similarly monitored and used to assist in the measurement of heat transfer coefficients at the top, sides, and bottom. All thermocouple signals were routed through a bank of rotary switches to a digital temperature readout.

Voltage profiles were mapped using probes made from 1/16 in. OD stainless steel welding rod inserted into polyethylene tubing with only the tip of the welding rod exposed. A bare copper wire running axially from the surface of the model fluid to the bottom of the tank served as a reference potential (artificial ground) in all voltage measurements. Voltage signals were routed through a bank of rotary switches to a voltmeter for readout.

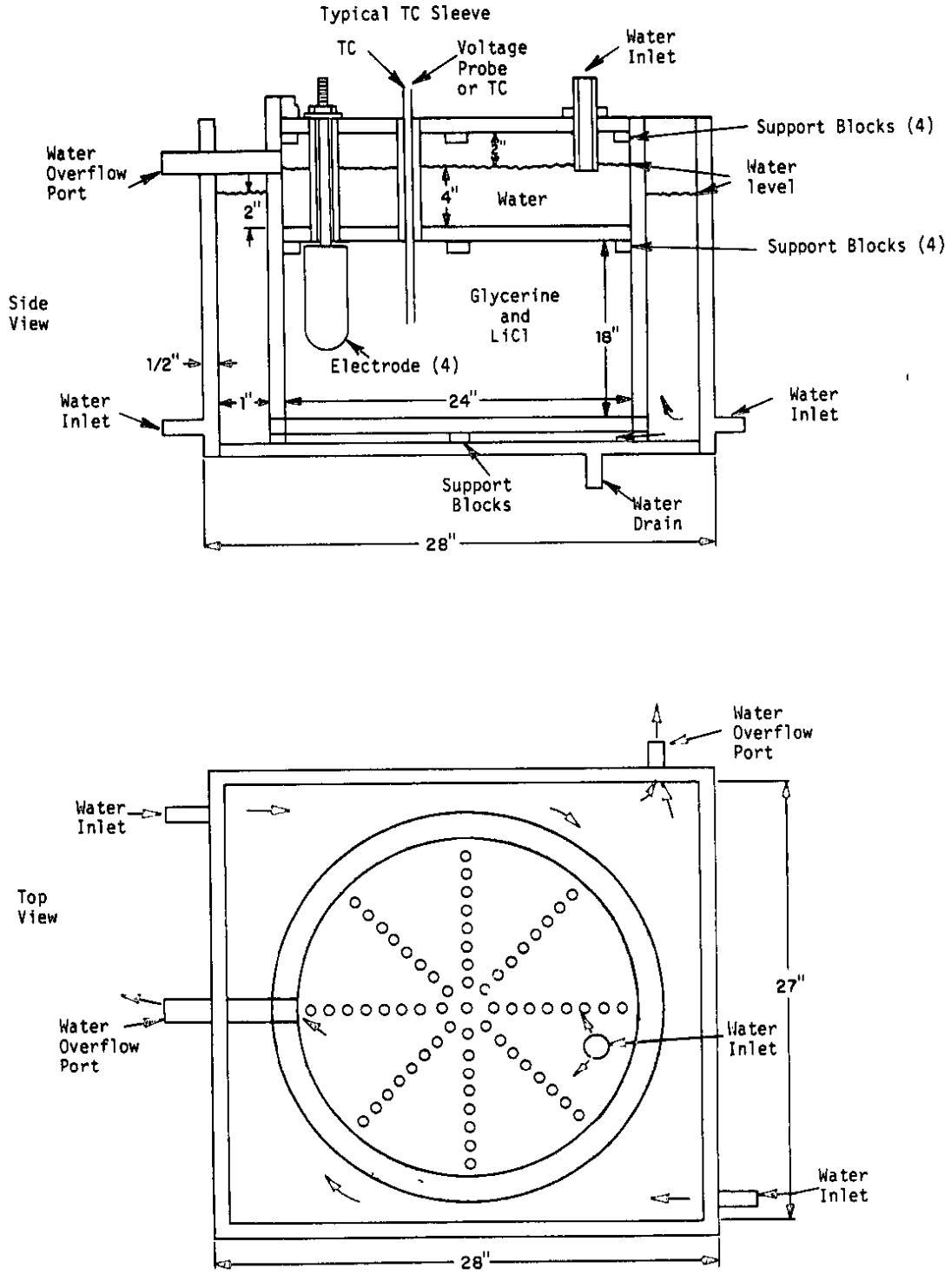

FIGURE 9. Plexiglas® Tank

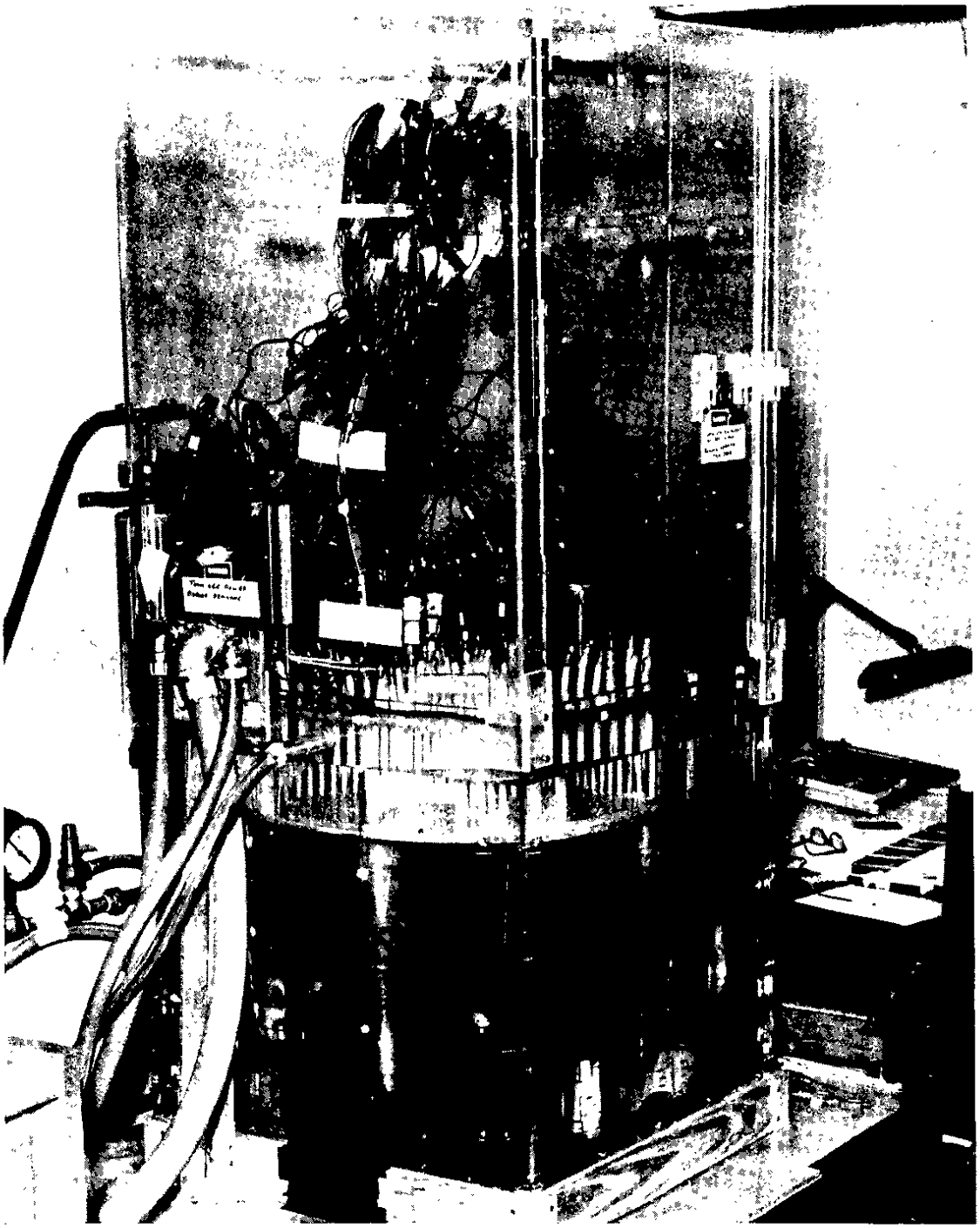

FIGURE 10. Model of Full-Scale Glass Melter

A simplified wiring diagram of the power supply to the electrodes is shown in Figure 11. The desired 90° phase separation between the potential applied to electrodes A-C and the potential applied to electrodes B-D was achieved as described previously. Resistor banks were used to vary the applied voltage to each electrode pair and thus control input power to the system. Since the resistivity of the model fluid decreases approximately exponentially with increasing temperature, temperature controllers were installed to interrupt power to the model if a preset temperature was exceeded. Control of the system was simple and straightforward.

To study the velocity profiles in the model, a light box was constructed using six rheostat-controlled, point source lamps† mounted in a sheet metal box. The top of the box was covered with one of four collimating slits (1/16 in., 1/8 in., 1/4 in., or 1/2 in.), which was in turn covered with a 1/4 in. thick plate of infared glass to reduce heat transmission from the light box to the model. A small instrument cooling fan was used to provide additional cooling for the point source lamps. The box was placed beneath the model and used to provide a narrow sheet of light passing up through the model in a vertical plane and illuminating tracer particles injected into the model fluid.

3. Operation

During startup, 208 volts was applied to each electrode pair to accelerate the attainment of operating temperature. Then the wiring configuration of Figure 11 was switched in to give the 90° phase shift between electrode pairs A-C and B-D. The resistor banks were used to stabilize the bulk operating temperature. No data was taken for at least 24 hours to allow the system to reach steady state. Thermocouples were monitored on the outside of the side walls, bottom, and top and inside the tank on the bottom, surface, and about two inches below the surface to ensure steady state was maintained and that the desired heat transfer boundary conditions were met.

Radial and azimuthal temperature profiles were taken at numerous axial levels in the tank, starting at the bottom and progressing upward. Axial temperature profiles were available from these data as well as specific individual axial temperature profiles.

---

† General Electric FCS Quartzline Lamp, 24 volts, 150 watts.

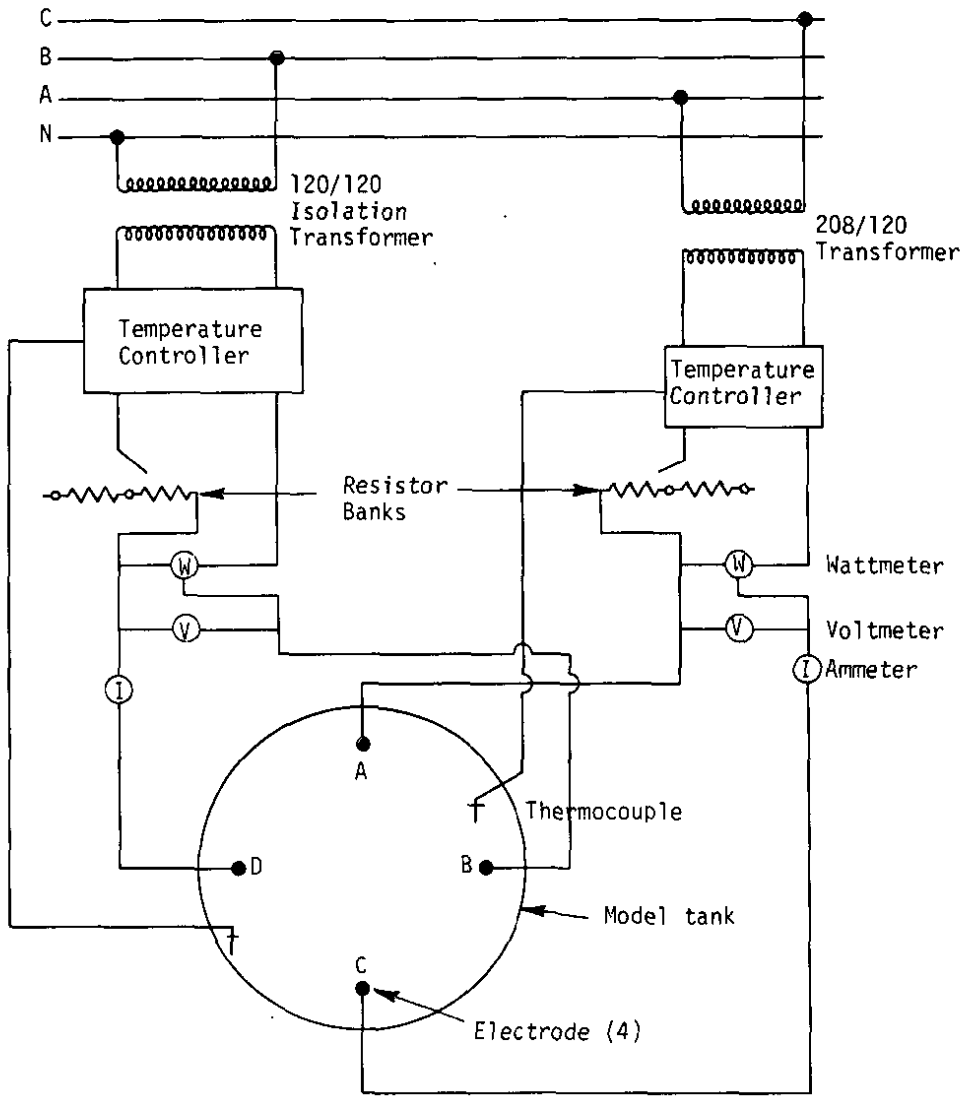

FIGURE 11. Power Supply to Model

Since the model fluid was electrically charged, it was necessary to cut off the power whenever the thermocouples were repositioned to avoid electrical shock. This led to a slight cooling of the model fluid which was generally compensated for by slightly increasing the power level just before a run was started and/or adjusting the cutoff point on the temperature controllers to maintain the desired bulk temperature. Bulk temperature fluctuations were thus held to 1 to 2°F.

Voltage profiles were taken in the same manner as the temperature profiles. All voltages were measured with respect to a bare copper wire running vertically from the surface to the bottom at r = 0.

To measure velocity profiles in the model it was necessary to select tracer particles that were neutrally buoyant, i.e., they must neither rise nor sink, but rather follow the natural convective patterns set up in the fluid. They also had to be insoluble, chemically inert, possess a different refractive index than the model fluid, and reflect light well.

Several ion exchange resins, plastics, etc. were tried, but anthracene ($C_{14}H_{10}$) seemed to work best. Particles in the range of 20 to 50 mesh were large enough to be tracked individually on photographic film, but were slightly buoyant, and would rise to the surface in 20 to 30 minutes. However, particles ground and sieved to <100 mesh were found to stay in solution for several days or more, and being slightly soluble, would eventually disappear. Particles this small could not be distinguished individually on film, but rather appeared (in sufficient concentration) like a small cloud. No effect of the anthracene on the physical properties of the model fluid could be measured, presumably because of its presence only in relatively small quantity.

Anthracene was prepared for injection into the model by mixing about 20 grams of <100 mesh particles in 250 mL of the model fluid. A 1/2 in. OD polyethylene tube was inserted through the top of the model down to the desired injection point and filled with the tracer mixture up to a level equal to that of the model fluid in the tank. After the tracer mixture in the tube reached thermal equilibrium with the model fluid, approximately another 5 to 10 mL of additional tracer mixture was added to the tube, which forced an equal amount out of the bottom of the tube into the model fluid. This resulted in a small spherical puff at the bottom of the injection tube whose movement could then be followed as a function of time. Alternatively, a line source of tracer particles was sometimes injected by slowly withdrawing the injection tube as the tracer mixture oozed out its bottom.

Movement of the tracer particles was recorded using a Polaroid† MP-4 camera and Polaroid† Type 55, ASA 50 film. It was necessary to completely darken the room, except for the vertical light sheet passing up through the model from the light box. Film exposure time was generally 10 to 30 seconds, while particle velocities were on the order of inches/hr.

† Trademark of Polaroid Corp., Cambridge, MA.

REFERENCES

1. R. B. Bird, W. E. Stewart, and E. N. Lightfoot. *Transport Phenomena*. John Wiley and Sons, Inc., New York (1960).

2. Ingrid Sanderud, et al. "Static and Dynamic Investigation by Model Experiments of an Electrically Heated Glass Furnace." *Glass Technology*, 16 (2) pp 39-45 (April 1975).

3. S. Kruszewski. "A Study on Models of the Effects of Operation and Design on the Glass Flow in Tank Furnaces." *Glass Technology*, Vol. 41 (1957).

4. J. Stanek, et al. "Flow of Glass in Furnaces Heated by Electricity." *Glass Technology*, Vol. 10, No. 2 (April 1969).

5. J. J. Noble, et al. "Mathematical and Experimental Modeling of the Circulation Patterns in Glass Melts." *Journal of Heat Transfer*, p. 149 (May 1972).

6. N. W. E. Curlet. "Experimental and Numerical Modeling of Three-Dimensional Natural Convection in an Exclosure." D. Sc. Thesis, Massachusetts Institute of Technology (March 1976).

7. B. Bansal. "Physical Modeling of All-Electric Furnaces." *IEEE Trans. on Industry Appl.*, Vol. IA-14, No. 1 (Jan/Feb 1978).

8. M. S. Quigley and D. K. Kreid. "Physical Modeling of Joule-Heated Ceramic Glass Melters for High-Level Waste Immobilization." USDOE Report PNL-2809, Pacific Northwest Laboratories, Richland, WA (March 1979).

9. L. A. Clomburg, Jr. "Mathematical and Experimental Modeling of the Circulation Patterns in Glass Melts." D. Sc. Thesis, Massachusetts Institute of Technology (August 1971).

10. J. Stanek. *Electric Melting of Glass*. Elevier Scientific Publishing Company, New York (1977).

11. R. T. Morrison and R. N. Boyd. *Organic Chemistry*. Allyn and Bacon, Inc., Boston (1965).